

ARTICLE

The Genetic Mechanism of Inertinite in the Middle Jurassic Inertinite-Rich Coal Seams of the Southern Ordos Basin

Dongdong Wang^{1*} Qiang Mao¹ Guoqi Dong¹ Shipeng Yang² Dawei Lv¹ Lusheng Yin¹

1. College of Earth Science and Engineering, Shandong University of Science and Technology, Qingdao Shandong, 266590, China

2. Shandong Institute of Geological Survey, Ji'nan Shandong, 250013, China

ARTICLE INFO

Article history

Received: 12 November 2019

Accepted: 28 November 2019

Published Online: 31 December 2019

Keywords:

Inertinite-rich coal

Wildfire events

Oxidation effects

Genetic mechanism

Jurassic Period

Ordos Basin

ABSTRACT

Inertinite is an important type of organic maceral in coal deposits, and also an important geological information carrier of coal forming environments. In the southern section of the Ordos Basin, the No. 4 inertinite-rich coal seam of the Middle Jurassic Yan'an Formation in the Binchang Coal field was selected as an example to study the genetic mechanism of the inertinite. In this study, the results obtained from experimental tests of coal rock, including principal and trace elements, stable carbon isotopes, scanning electron microscopy, inertinite reflectance, sporopollen and free radical retorting methods, were analyzed. Then, the findings were combined with the previous understanding of the oxygen content in the atmosphere and ground fire characteristics, in order to discuss the genesis mechanism of inertinite in the No. 4 coal seam. The obtained research results were as follows: (1) During the coal forming period of the No. 4 coal seam, the overall climate had been relatively dry. There were four relatively dry-wet climate cycles in the No.4 coal seam, which were controlled by the eccentricity astronomical period. The inertinite content were relatively high during the dry periods; (2) The temperature range suitable for microorganism activities during the oxidation processes was between 0 and 80 °C . The simulation results of the free radical concentrations showed that the maximum temperature of fusain in the No. 4 coal seam during the process of coalification had not exceeded 300 °C , which was significantly higher than the temperature range of microorganism activities. Therefore, these were not conducive to the activities of microorganism and formation of inertinite during the coal-forming period; (3) The genesis temperature of the inertinite in the No. 4 coal seam was calculated according to the reflectance of the inertinite, which was lower than 400 °C . This result supported the cause of wildfire of the inertinite and reflected that the type of wildfire was mainly ground fire, along with partially surface fire. Moreover, the paleogeographic location, climatic conditions, atmospheric oxygen concentration, etc. of the study area showed that the conditions for wildfire events were in fact available; (4) There were dense and scattered fusinite observed in the No. 4 coal seam, and the thickness of cell walls were found to differ. It was speculated that this was related to the type of wildfire, combustion temperatures, combustion timeframes, and different initial conditions of the burned objects during the coal forming periods.

*Corresponding Author:

Dongdong Wang,

College of Earth Science and Engineering, Shandong University of Science and Technology, Qingdao Shandong, 266590, China;

Email: wdd02_1@163.com

1. Introduction

Inertinite-rich coal deposits have been widely developed and are distributed throughout the world, among which Gondwana coal is the most representative type. Gondwana coal mainly formed during the Permian, Triassic, and Jurassic in Europe, North America, East Australia, South Africa, India, and other regions. Among those period, the Permian is known to have had the highest development of Gondwana coal containing very high content levels of inertinite (up to 85%), and mainly composed of semifusinite and inertodetrinite^[1-9]. The Middle- Jurassic coal formations of northwestern China are also rich in inertinite, with the majority of the coal deposits having more than 35% content levels, and even more than 80% in some case. It has been determined that the content levels of transitional components, such as semifusinite and inertodetrinite, generally range between 10% and 20%^[4,10-17].

However, the genesis of inertinite in coal has been disputed for a long period of time^[1,2,18-19]. As early as the 20th century, there have been two main genetic views: primary inertinite and secondary inertinite^[1,20].

The primary inertinite is a product resulting from a series of oxidation processes of peat, such as strong oxidation and alteration, dehydration, oxygen loss, hydrogen loss, carbon rich, and so on during in the peat formation stage. This is commonly referred to as oxyfusinite. It is characterized by poorly preserved cell structures and sometimes intercellular layers can be seen. Also, wedge-shaped oxidation cracks are generally developed in the cell walls^[21].

Gondwana inertinite-rich coal was mainly formed under cold temperate climate conditions in the sub-polar climate zones and the surrounding areas, with alternating dry and rainy seasons^[2]. The coal formed peat swamps were very wet and anoxic during the summer months, while suffering drought conditions during the winter under oxidation environmental conditions^[2]. The presence of Gondwana inertinite-rich coal deposits indicate relatively dry climatic and strong peat oxidation conditions^[4]. Harvey and Dillon^[21] and Phillips et al.^[22] also determined that the coal (coal core) of the Pennsylvania Formation located in Illinois (US) had been formed under drier climate conditions, and had a relatively high content of fusinite^[22-23]. Hunt and Smyth^[23] believed that the inertinite-rich coal in the Permian Craton Basin (Cooper Basin and Galilee Basin) of Australia had formed due to high accumulation in freshwater swamps and the widespread oxidation of peat resulting from low settlement rates^[24]. The Jurassic inertinite-rich coal deposits in northwestern China were also formed under relatively dry climate conditions^[17],

during which the peat swamp surfaces were oxidized for long periods of time during the coal formation period^[25-26]. Subsequently, these factors were the reason for the high content levels of oxidized fusinite in the coal seams of the area.

In addition, the peat was transported and redeposited again following deposition, and parts of peat had been oxidized to produce inertinite with low reflectance^[27]. Moore^[27] reported that some researchers had proposed an alternate secondary genesis of the fungi in inertinite^[28]. During the peat formation stage, the remaining plants were biochemically decomposed under the actions of fungi in weak oxidation environmental conditions. In addition, coarse grains and inert debris were the direct products of the biochemical decomposition processes^[28]. Styan and Bustin^[28] believed that when the xylem of plants is decomposed by dry rot fungi, it can form oxidized fusinite with cell very fuzzy structures^[29]. Li^[4] found that for the Middle Jurassic dried and oxidized low water level raised moorlands in northwestern China, the peat surface layers were exposed to the weak oxidation conditions of atmospheric weathering, and considered that fungi alternating effect were one of the genetic mechanisms of the inertinite formation in the region^[4]. Hower et al.^[17] believed that fusinite could be the result of the oxidative degradation of fungi or microorganisms^[18].

The inertinite of the secondary genesis, which is generally represented by pyrofusinite, is known to have formed as a result of forest fires or peat swamp fires. When such fires occurred, plant tissues were charred and carbonized under high temperatures, displaying clear cell structures, thin cell walls, and homogenized cell walls, with no observable intercellular layers^[30]. Pyrofusinite is considered to be the product of the incomplete combustion of plants during wildfire events^[30], and often show lenticular and thin-layer output in coal seams. In addition, in the cases where the partially humified wood was in a moist state and had burned less completely, fire burnt semi-fusinite with slightly thick cell walls had been formed^[21].

Teichmuller (1961) found that the peat in the peat swamps of Holland was burned by fire and then carbonized to form pyrofusinite, and peat coke had accumulated in situ^[31]. Austen et al.^[31] used an electron spin resonance method to determine that some of the fusinite in the Carboniferous coal of Europe and America had been affected by high temperatures before accumulation occurred, which was obviously a type of fusinite formed by wildfires^[3]. Singh and Shukla^[3] proposed the theory that the influences of wildfire events had significantly increased the inertinite content of the Gondwana coal. Many of the performed plant carbonization experiments showed that

the carbonization temperatures were directly proportional to the reflectance of the inertinite^[33-36]. Therefore, according to the reflectance of the inertinite and the palynological data, combustion temperatures can be estimated and the fire types (crown fires, surface fires, and ground fires) can be accurately classified^[37]. The inertinite reflectance of the Carboniferous bituminous coal in the Silesia Basin was determined to have changed greatly, which reflected the existence of diversified types of wildfires in the region, as well as the characteristics of surface fires^[38].

During wildfire events, lightning strikes may be the main fire source which produce charcoal. Therefore, it can be said that the presence of polycyclic aromatic hydrocarbons (PAHs) and heterogeneous charcoal in strata is evidence of wildfire activity^[37]. For example, such evidence of wildfires have been found in the Permian of the southern continent of Gondwana^[3,5-9]; Permian of northern China^[39-42]; upper Paleozoic erathem of Central Europe^[43-47]; and middle and upper Permian in Brazil^[8-9]. Scott^[47], Scott and Glasspool^[48] believed that the so-called inertinite of non-combustion origin, such as semi-fusinite, can be explained by the low-temperature combustion, short-term combustion, and the different initial conditions of the combusted objects^[48-49].

Therefore, from the perspective of its global evolution, the distribution of inertinite in the strata from Silurian to Neogene humic coal clearly shows that the global evolution trend of inertinite content in coal was mainly affected by the changes in climate conditions, sedimentary environments, and local regional tectonic characteristics. The overall pattern of stratigraphic distribution supports the view that incomplete combustion was the main source of the inertinite in coal. These findings indicate that the long-term changes in the atmospheric oxygen content levels could be effectively used to explain the global changes in the inertinite distributions. Meanwhile, the response rates affected by the different settlement and climate conditions were considered to have controlled the regional and local variations of the percentages of inertinite in the coal deposits^[50].

It can be seen that there are still major differences in the genesis theories of inertinite in coal. In this study, a coal seam of the Middle Jurassic Period in the Yan'an Formation, located in the southern section of China's Ordos Basin, was taken as an example for the purpose of examining the genetic mechanism of the inertinite in coal in order to further enrich the basic theories of coal geology.

2. Geological Background

The Ordos Basin is a large Meso Cenozoic depression basin situated in north central China. It is known to be rich

in coal, petroleum, natural gas, uranium, and other mineral resources, and is an important comprehensive energy base for China. Among China's energy sources, coal production continues to account for approximately one-quarter of the energy supply for the entire country. In particular, the Middle Jurassic coal deposits are of major importance due to their abundant coal resources.

The Ordos Basin is surrounded by the Qinling Mountain Range, Liupan Mountain, Helan Mountain, Daqing Mountain, and Luliang Mountain. In addition, the Fen-wei Basin is located south of the Ordos Basin, and its southern boundary is approximately located in the Weihe River Valley. It is bordered by the Yinchuan and Liupanshan Basins in the west, and its western boundary is located on the line of western foot of Helan Mountain-Qingtongxia-Guyuan. The Ordos Basin is adjacent to the Hetao Basin in the north, and its northern boundary is approximately located on the line of Wula Mountain -Daqing Mountain. Its eastern boundary had become seriously corroded in the later period of its development and is estimated to be located east of the Datong-Yima line (Figure 1). The Dafosi Coal Mine of the Binchang Coal Field is located in the southwestern section of the Ordos Basin. Several ancient uplifts can be observed in the coal field which were formed during the coal formation period. These ancient uplifts are without stratigraphic deposition, which to some extent may have provided sediment sources. The Dafosi Coal Mine is located in the south region of the Binchang Coal Field (Figure 1c).

The coal bearing strata of the Binchang Coal Field includes the Yan'an Formation of the Middle Jurassic Period. The formation mainly consists of sandstone, mudstone, coal seams, and so on. It has been divided into five sections from the bottom to the top, which are referred to as the Yan 1 to Yan 5 Sections. A developed coal seam group is located in the upper part of each section, while the lower parts of each section are dominated by sandstone deposition. It can be seen that within the basin, the preservation degree of strata in the Yan'an Formation gradually improves from the southeast to the northwest. The southeastern and southern strata of the basin are seriously denuded, with only the lower Yan 1 Section retained in the local area. The upper part of the Yan'an Formation of the Dafosi Coal Mine in the Binchang Coal Field is seriously eroded, with the middle and upper strata eroded to various degrees in different areas. The coal seams of the Yan'an Formation of the Dafosi Coal Mine are generally thick. The average single layer thickness of the No. 4 coal seam of ZK1 and ZK2 (near ZK1) examined in this study were determined to be 11.3 m and 8.1m, and the main coal forming environments were river swamp and lakeside swamp.

The body of the No. 4 coal seam in the Yan 1 Section of the Binchang Coal Field was observed to be black-brown to black in color, with dark brown colored streaks characterized by a pitchy luster. Ragged-conchoid fractures were observed, as well as both thin band-linear strip structures and massive-layered structures. The No. 4 coal seam is mainly composed of dull coal, followed by bright coal, and low quantities of specular coal. Among the types of coal, the endogenetic fractures in the specular coal were found to be relatively developed, followed by the bright coal deposits. In ZK1, the average content of organic maceral in the No. 4 coal seam was determined to be 89.19%; The average content of total minerals was 10.81%; In the organic macerals, the average content of inertinite was found to be 50.74%, the average content of vitrinite was 30.73%, the average content of liptinite was 7.72%, and the average content of mineral was 10.8%; The maximum reflectivity of vitrinite of No. 4 coal seam was 0.64-0.75%, with an average of 0.71%, which is low-metamorphism bituminous coal.

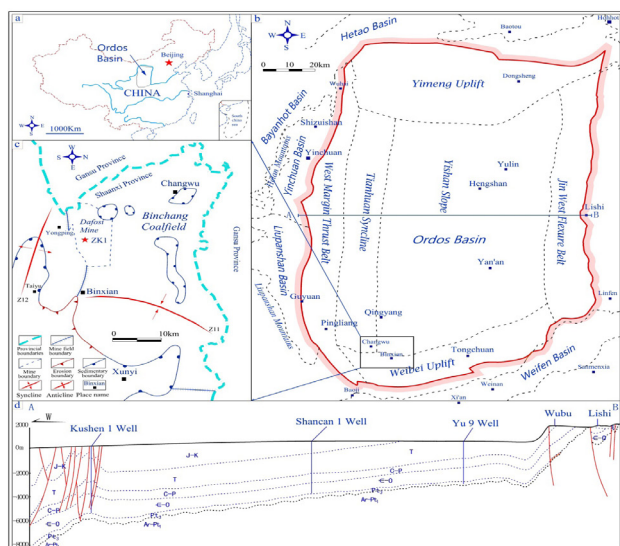


Figure 1. Geological map of Ordos Basin and Binchang Coal Field ^[51]

3. Samples and Methods

The single-layer thickness of the No. 4 coal seam in the Yan 1 Section of well ZK1 in the Binchang Coal Field was 11.3 m. This study selected 20 coal samples from the No.4 coal seam of ZK1, which were systematically collected at an equal spacing of 0.5 m. The top to bottom serial numbers were ZK1-1 to ZK1-20, respectively. And another well ZK2 is near the ZK1, the No.4 coal seam was 8.1 m, in which 15 samples were collected with equal spacing of 0.5m. The top to bottom serial numbers were ZK2-1 to ZK2-15, respectively. The samples were analyzed in the current study using anthracology; inertinite reflectance

measurements; stable carbon isotope analyses of the organic matter; analyses; and scanning electron microscopy.

For coal rock analyses and inertinite reflectance measurements, a Zeiss microphotometer (HD-MY5000) was adopted. This study referred to the *Classification of Coal Minerals* (ICCP System, 1994) for the appropriate coal rock analysis standards. In addition, for the determination of the inertinite reflectance, three standard samples (0.590%, 0.904%, and 1.719%) were used for the calibration process. The *Microscopical Determination of the Reflectance of Vitrinite in Coal* (GB/T 6948-2008) was referenced for the complete description of the analysis method and process requirements.

An isotopic mass spectrometer (MAT251/252) was used for the stable carbon isotope analyses of the organic matter. This study referred to the *Determination of Organic Carbon Stable Isotopic Component - Isotopic Mass Spectrometry* (GB/T 18340.2-2010) for the analysis method and process requirements.

In the present study, a plasma mass spectrometer (ICP-MS, X Series 2) was used for the analysis of the major and minor elements, and referred to the *Method for Chemical Analysis of Silicate Rocks - Part 30: Determination of 44 Elements* (GB/T 14506.30-2010); *Method for Chemical Analysis of Silicate Rocks - Part 14: Determination of Ferrous Oxide Content* (GB/T 14506.30-2010); and the *Method for Chemical Analysis of Silicate Rocks - Part 28: Determination of 16 Major and Minor Elements Content* (GB/T 14506.28-2010) for the appropriate analysis methods and processes.

A scanning electron microscope (SEM) was used for the SEM analysis in this study. The analysis method and process were in accordance with the *Analytical Method of Rock Sample by Scanning Electron Microscope* (SY/T 5162-1997).

4. Results

Based on the analysis results of the No. 4 coal seam in the Yan 1 Section of the Binchang Coal Field, it was determined that the inertinite accounted for between 28.1% and 81.7% of the total rock masses, with an average content of 40.7%. In addition, it accounted for between 32.3% and 86.1% of the total content of organic components, with an average content of 45.6% (Table 1). It was observed that the inertinite content and vitrinite/inertinite ratio displayed four periodic cycles in the vertical direction, which were assumed to reflect the dry and wet climate changes which had occurred in the region (Figure 2).

Then, by analyzing the scanning electron microscope observations of the coal samples, it was found that there were two major types of fusinite in the inertinite. The first

type was dispersed throughout the coal, with the characteristics of relatively poorly preserved cell structures and very thick cell walls, as shown in Figure 3-F1. The second type was characterized by thin-layers or lenticular distributions within the coal, with the fusinite being heavily concentrated in various areas. It was found that the cell walls thin, with well-preserved cell structures. However, the second type appeared to be relatively broken, as shown in Figure 3-F2.

Table 1. The maceral types and contents and the vitrinite maximum reflectivity ($V-R_{max}^0$, %) of No.4 coal seam of Yan'an Formation in the south of Ordos Basin (%)

No	Vitrinite	Inertinite	Liptinite	Total organic matter	Clay	Carbonate	Sulfide	Oxide	$V-R_{max}^0$, %
ZK1-1	46	26.9	13.5	86.4	1.2	-	0.6	11.8	0.75
ZK1-2	27.9	40.3	9.2	77.3	0.6	18.6	1.2	2.3	0.72
ZK1-3	37.9	35.8	5.5	79.3	0.6	10.9	5.7	3.4	0.73
ZK1-4	28	42.2	6	76.3	1.7	19.7	0.6	1.7	0.72
ZK1-5	39.2	42.3	7.1	88.6	1.1	9.1	-	1.1	0.7
ZK1-6	26.7	59.6	10.2	96.5	1.8	0.6	-	1.2	0.69
ZK1-7	33.1	51.7	8.7	93.5	3.5	-	-	2.9	0.72
ZK1-8	52.3	28.1	6.6	87	2.2	9.7	0.5	0.5	0.7
ZK1-9	25.7	62.6	6.8	95.1	2.7	-	-	2.2	0.73
ZK1-10	18.7	43.8	4.8	67.3	1.3	24.4	6.4	0.6	0.68
ZK1-11	40.6	44.8	5.7	91.1	3	5.9	-	-	0.64
ZK1-12	32.9	54.6	10	97.5	1.9	-	-	0.6	0.69
ZK1-13	48	31.3	5.2	84.5	0.6	5.7	9.2	-	0.69
ZK1-14	45.7	44	8.5	98.2	1.2	-	-	0.6	0.68
ZK1-15	30.4	53.5	12.1	96	2	1	0.5	0.5	0.69
ZK1-16	6.3	80.4	10	96.7	2.2	-	-	1.1	0.7
ZK1-17	12.4	75.2	9.9	97.5	2.2	-	-	0.3	0.75
ZK1-18	12.4	81.7	0.8	94.9	3.8	-	-	1.3	0.73
ZK1-19	4.7	73	10.7	88.4	3.4	4.5	0.7	3	0.72
ZK1-20	45.6	43	3	91.6	-	7.6	0.8	-	0.73
AVG	30.7	40.7	7.1	89.2	1.95	9.81	2.6	2.1	0.71

Furthermore, based on the analysis results of the principal and trace elements, and carbon isotopes (Table 2) of the No. 4 coal seam in the Yan 1 Section of the Binchang Coal Field, it was determined that the typical elements, minerals (assemblages), carbon isotopes, and so on, which reflected the climatic changes, had displayed certain vertical regularities (Figures 3 and 5). It was considered in the study that the observed patterns had roughly reflected four cycles of dry and wet periods which had occurred during the paleoclimate changes in the region.

The measurement results of the reflectance of inertinite

in 9 coal samples obtained from the No. 4 coal seam of the Yan 1 Section in the Binchang Coal Field revealed that the reflectance of inertinite of the No. 4 coal seam was mainly concentrated within the range of 1.1 to 2.53%, with individual points lower than 1.1% and higher than 2.5%. The average reflectance of the inertinite was determined to be 1.64%, with a standard deviation of 0.2 to 0.29. Therefore, the reflectance of the inertinite distribution was relatively concentrated (Table 3). The reflectance distributions of the inertinite of the different samples were found to vary, with some relatively concentrated and some scattered, reflecting a variety of causes (Figure 6).

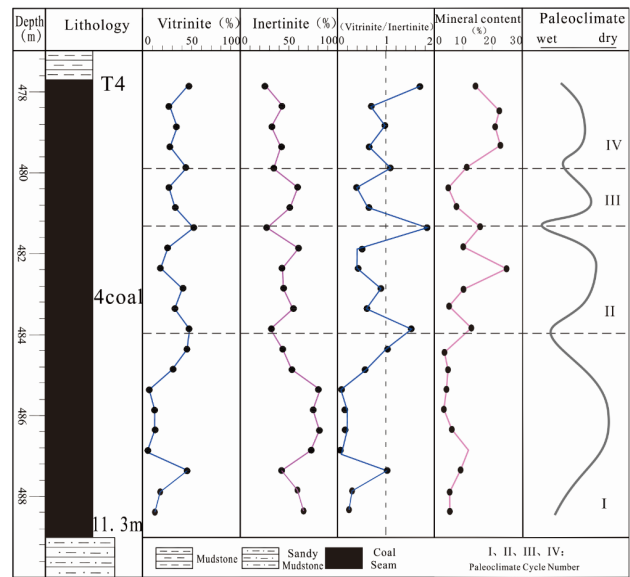


Figure 2. Relationship of vertical changes between coal maceral and paleoclimate cycles in No.4 coal seam of Yan 1 Section in ZK1, Binchang Coal Field

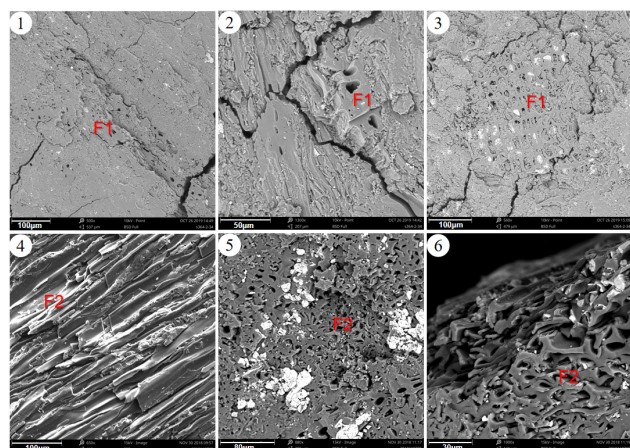


Figure 3. Fusinites under SEM in No.4 coal seam of Yan 1 Section in ZK1, Binchang Coal Field

Note: F1- fusinite with thick cell walls; F2- fusinite with thin cell walls.

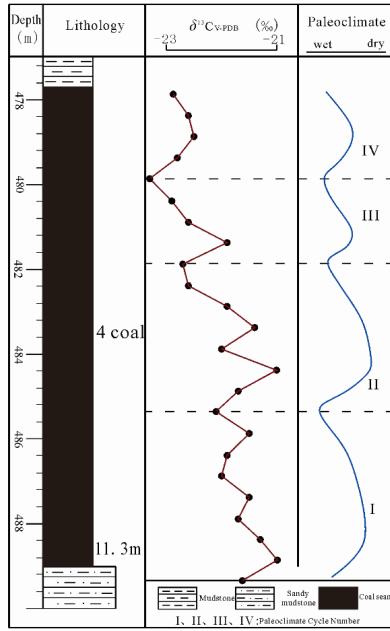


Figure 4. Relationship between carbon isotopic vertical changes and paleoclimate cycles in No.4 coal seam of Yan 1 Section in ZK1, Binchang Coal Field

Table 3. The inertinite reflectance (I-R°, %) of No. 4 coal seam of Yan 1 section in ZK2, Binchang Coal Field

No.	I-R° _{min} , %	I-R° _{max} , %	I-R° _{avg} , %	Number of samples	Standard Deviation
13	1.25	2.53	1.60	51	0.23
15	1.21	2.14	1.65	58	0.29
17	1.33	2.3	1.79	53	0.29
19	0.91	2.05	1.45	51	0.23
21	1.22	4.54	1.74	53	0.29
23	1.3	2.18	1.65	45	0.2
25	1.17	2.23	1.59	54	0.29

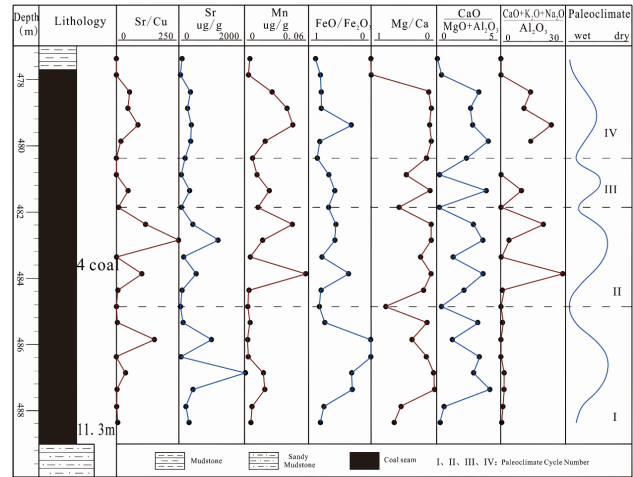


Figure 5. Relationship between characteristic elements (mineral ratios) vertical changes and paleoclimate cycles in No.4 coal seam of Yan 1 Section in ZK1, Binchang Coal Field

Table 2. The mineral (element) contents and carbon isotopes of No.4 coal seam of Yan 1 Section in ZK1, Binchang Coal Field

No.	Sr	Cu	Sr/Cu	MnO	Mn	FeO	Fe₂O₃	FeO/Fe₂O₃	Mg	Ga	Mg/Ga	Al₂O₃	MgO	CaO	Na₂O	K₂O	CaO/(MgO+Al₂O₃)	(CaO+K₂O+Na₂O)/Al₂O₃	δ¹³Cv-PDB
	μg/g	μg/g		%	%	%	%		%	%	%	%	%	%	%	%			‰
1	103.00	53.10	1.94	0.007	0.005	0.630	0.705	0.894	0.211	0.059	3.552	17.180	0.351	0.083	0.340	1.500	0.079	0.128	-
2	53.20	26.60	2.00	0.005	0.004	0.150	0.185	0.811	0.109	0.101	1.078	4.350	0.181	0.141	0.203	0.107	0.385	0.113	-22.1
3	347.00	6.22	55.79	0.033	0.026	2.060	2.560	0.805	1.158	10.771	0.108	1.100	1.930	15.080	0.121	0.012	3.359	1.875	-22.5
4	267.00	5.30	50.38	0.052	0.040	2.650	3.350	0.791	0.672	8.436	0.080	1.130	1.120	11.810	0.126	0.016	2.642	1.117	-22.6
5	393.00	4.43	88.71	0.059	0.046	1.260	4.130	0.305	1.194	12.343	0.097	0.734	1.990	17.280	0.120	0.012	2.824	2.891	-21.9
6	370.00	17.10	21.64	0.025	0.019	1.690	2.000	0.845	0.786	9.636	0.082	0.992	1.310	13.490	0.126	0.015	4.076	1.463	-22.7
7	204.00	52.30	3.90	0.009	0.007	0.390	0.452	0.863	0.202	1.371	0.147	1.330	0.337	1.920	0.142	<0.010	2.433	0.000	-22.6
8	75.90	43.80	1.73	0.015	0.012	0.670	0.985	0.680	0.114	0.250	0.456	1.750	0.190	0.350	0.169	0.016	0.298	0.214	-21.9
9	298.00	5.94	50.17	0.030	0.023	1.060	1.790	0.592	0.750	8.536	0.088	1.280	1.250	11.950	0.132	0.019	3.931	1.095	-21.4
10	82.10	5.90	13.92	0.017	0.013	0.660	1.050	0.629	0.110	0.192	0.571	1.670	0.183	0.269	0.173	0.011	0.218	0.220	-22.0
11	424.00	3.65	116.16	0.060	0.046	2.360	4.240	0.557	0.996	12.321	0.081	0.871	1.660	17.250	0.135	0.012	2.924	2.075	-20.1
12	1201.00	4.52	265.71	0.022	0.017	0.810	1.400	0.579	0.367	5.229	0.070	1.970	0.612	7.320	0.130	0.028	3.638	0.391	-21.7
13	128.00	50.40	2.54	0.007	0.005	0.170	0.219	0.776	0.085	0.349	0.244	1.450	0.142	0.489	0.129	0.013	1.355	0.196	-22.1
14	551.00	5.23	105.35	0.075	0.058	1.310	3.720	0.352	1.080	14.214	0.076	0.695	1.800	19.900	0.155	0.018	3.605	2.839	-21.5
15	94.90	8.44	11.24	0.005	0.004	0.140	0.175	0.800	0.095	0.511	0.185	1.350	0.158	0.716	0.127	0.017	2.150	0.224	-21.9
16	118.00	59.90	1.97	0.007	0.005	0.260	0.317	0.820	0.101	0.129	0.784	1.910	0.169	0.181	0.158	0.028	0.372	0.186	-22.0
17	103.00	51.50	2.00	0.007	0.005	0.120	0.163	0.736	0.116	0.836	0.139	2.150	0.193	1.170	0.151	0.013	3.287	0.166	-21.5
18	1005.00	6.51	154.38	0.004	0.003	<0.10	0.113	0.000	0.097	0.246	0.394	1.760	0.162	0.345	0.185	0.015	1.255	0.206	-21.7
19	68.80	57.50	1.20	0.005	0.004	<0.10	0.110	0.000	0.101	0.675	0.149	3.910	0.168	0.945	0.128	0.059	3.399	0.091	-21.3
20	2083.00	53.70	38.79	0.023	0.018	0.500	1.630	0.307	0.160	3.943	0.041	3.760	0.267	5.520	0.145	0.034	2.910	0.119	-20.8
21	421.00	60.80	6.92	0.024	0.019	0.590	1.990	0.296	0.124	6.571	0.019	5.600	0.207	9.200	0.157	0.140	4.188	0.090	-21.6
22	187.00	30.40	6.15	0.009	0.007	0.800	1.040	0.769	0.153	0.274	0.558	21.620	0.255	0.384	0.386	0.646	0.297	0.060	-
23	412.00	31.20	13.21	0.007	0.005	0.690	0.819	0.842	0.122	0.169	0.723	20.500	0.203	0.236	0.354	0.534	0.231	0.053	-

5. Discussion

5.1 Relationship between the Climatic Conditions and the Inertinite Content Levels during the Coal Formation Periods

In regard to the genesis of the inertinite (particularly fusinite), regardless of whether it had been an oxidation or wildfire genesis, it was considered that relatively dry conditions were favorable for the formation of inertinite.

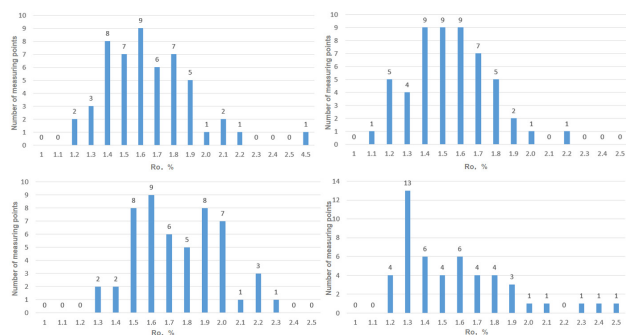


Figure 6. The inertinite reflectance distribution of No. 4 coal seam of Yan 1 Section in ZK2, Binchang Coal Field

(1) Ancient plants reflect the dry and wet changes of the ancient climate

The sporopollen in the No. 4 coal seam of the Yan 1 Section in the Binchang Coal Field had mainly developed as a palynological assemblage of *Classopollis-Cyathidites* minor. The content of the gymnosperm pollen was observed to be higher than that of the pteridophyte spores, and was characterized by high content levels of *Classopollis* pollen. The *Cycloidites minor* spores also accounted for an important proportion, which reflected the fact that the main coal forming plants were pteridophytes and gymnosperms^[25]. It is generally believed that the parent plants of *Classopollis* are mainly Cheirolepidiaceae, which usually occur under hot and dry climatic conditions^[52-53], but can also adapt to humid climates^[54]. The spore parent plants of the *Cyathidites minor* are generally considered to be Cyatheaceae and fernaceae (part), which are known to mainly grow under humid tropical and subtropical conditions^[55]. The development of the plant communities during the formation periods reflected that the coal forming periods had mainly experienced warm temperate subtropical climatic conditions. The characteristics of the sporopollen and spore assemblages of the ancient plants also reflected the complexity of the paleoclimate environment in the coal forming periods of the No. 4 coal seam in the Yan 1 Section, which had experienced approximately four cycles of dry and wet climate changes^[25].

(2) Compositions of the coal reflecting the changes in the dry and wet paleoclimate

The characteristics of coal organic macerals are

known to be closely related to the temperature and humidity levels of the paleoclimate. For example, the wetter the climate is, the more fully the plant remains will be able to decompose to form vitrinite-rich coal seams. In contrast, the drier the climate is, the more easily inertinite-rich coal seams will be formed^[56-57]. Therefore, it can be inferred that vitrinite is formed by gelation under the conditions of overlying water reductions, and inertinite is formed by fusinization under dry and hot oxidation marsh environmental conditions^[57]. If a peat swamp is a micro-environment with a high-water level, overlying water, and humidity, the formed peat will be transformed into coal vitrinite at a high percentage. Otherwise, if the water level of a peat swamp is low, the micro-environment will be generally dry, and the final coal inertinite formation will be high^[1,58]. In the present study, in accordance with the different genetic relationships among the macerals, and by using their statistical values, several parameters were introduced in the experimental processes in order to more intuitively reflect the genetic characteristics of the coal seam^[59]. Among the introduced parameters, the size of the vitrinite/inertinite ratio (V/I, also known as the moisture coefficient) in the coal was determined to accurately reflect the degrees of moisture or dryness of the peat swamps during the coal formation periods^[60-61]. The warm and humid paleoclimate was considered to be related to the percentage content and V/I ratio of the vitrinite and inertinite. Therefore, when the ratio of vitrinite to inertinite was greater than 1, it was indicated that the climate conditions had been warm and humid. However, when the ratio of vitrinite to inertinite was less than 1, it was indicated that the climate conditions had been hot and dry. Moreover, in accordance with the change trends of vitrinite content, inertinite content, and vitrinite/inertinite ratio, four wet-to-dry paleoclimate cycle changes were successfully identified in the No. 4 coal seam of the Yan 1 Section of the Binchang Coal Field. The content of inertinite was observed to be higher during the dry climatic periods (Figure 2).

(3) Characteristics of the elements and carbon isotopes reflecting the dry and wet changes of the paleoclimate

According to previous related research results, the main trace elements of the hygrophilous type are Cr, Ni, Mn, Cu, Fe, Ba, Br, Co, Cs, Hf, Rb, Sc, and Th. Meanwhile, the main trace elements of the xerophilous type are Sr, Pb, Au, As, Ca, Na, Ta, U, Zn, Mg, Mo, and B^[62]. When the content level of the element Sr is more than 20 $\mu\text{g/g}$, dry and hot climate conditions are inferred. In addition, when the content level is less than 0.15 $\mu\text{g/g}$, this tends to reflect a wet climate. In addition, when the content level of the

element Mn is more than 0.15 $\mu\text{g/g}$, a dry and hot climate is reflected, and when it is less than 0.15 $\mu\text{g/g}$, wet climate conditions can be assumed. When the ratio of Sr/Cu is larger than 10, a dry and hot climate environment is indicated. However, when it is less than 10, the climate conditions can be assumed to have been wet^[63-64]. It has been found that the current studies of paleoclimate using minor elements are too singular. Therefore, the ratio changes of the macro-elements, with characteristics indicating their meanings, were discussed in this research study. Generally speaking, Mg/Ca ratios greater than 0.5 reflect warm and humid climate conditions, and Mg/Ca ratios less than 0.5 reflect dry climate conditions^[65]. Furthermore, FeO/Fe₂O₃ ratios greater than 0.7 tend to reflect wet climate conditions, and FeO/Fe₂O₃ ratios less than 0.7 indicate dry environments^[66-67]. It has also been determined that ratios of CaO/(MgO+Al₂O₃) which are greater than 0.6 indicate warm climate conditions. Meanwhile, ratios of CaO/(MgO+Al₂O₃) which are less than 0.6 reflect cold climatic conditions. As further indicators of climate conditions, (CaO+K₂O+Na₂O)/Al₂O₃ ratios greater than five tend to reflect a dry climate, while (CaO+K₂O+Na₂O)/Al₂O₃ ratios less than five indicate a wet climate^[68]. In regard to the No. 4 coal seam in the Yan 1 Section of the Binchang Coal Field, according to the change trends of element content levels and ratios, it was identified that the coal seam had experienced four paleoclimate cycles of humidity and dry. The paleoclimate cycles are labeled by occurrence as I, II, III, and IV successively, from early to late. The No. 4 coal seam was determined to have a thickness 11.30 m, with the average thickness of each climate cycle determined to measure 2.83 m (Figure 4).

The $\delta^{13}\text{C}$ value of the organic carbon isotopes in a coal seam can potentially represent the temperature and humidity conditions during peat deposition. It has been found that such climate factors as humidity and temperature have important influences on the carbon isotope compositions of plants^[69]. Therefore, the $\delta^{13}\text{C}$ has a negative correlation with rainfall. That is to say, with increases in rainfall, the $\delta^{13}\text{C}$ value tends to decrease (lightens). However, in more arid environments, plants tend to adjust their stomatal resistance in order to avoid excess water evaporation, resulting in decreases in CO₂ concentrations within cells and changes in the $\delta^{13}\text{C}$ value^[69]. Under certain conditions, such as plant species and atmospheric compositions, dry and hot climatic conditions will be conducive to the enrichment of ¹³C in plants, and the $\delta^{13}\text{C}$ value of the coal-forming plants will be on relatively high. In contrast, wet and warm climatic environments are not conducive to the enrichment of ¹³C in plants, and the $\delta^{13}\text{C}$ value of the coal-forming plants will tend to be higher^[70]. In other

words, with increased temperature levels, when the value of the $\delta^{13}\text{C}$ becomes higher, paleoclimate changes from wet to dry heat are indicated. Meanwhile, when the value of the $\delta^{13}\text{C}$ becomes reduced, it is indicated that the paleoclimate changes are from dry heat to wet conditions. In the present study, the obvious negative and positive migration trends of the $\delta^{13}\text{C}$ in the No. 4 coal seam of the Yan 1 Section in the Binchang Coal Field revealed the transformations of the paleoclimate from dry to humidity, and from humidity to dry. Therefore, it was determined that the sedimentary period of the No. 4 coal seam experienced four cycles of humidity and dry paleoclimate evolution (Figure 3).

(4) Milankovitch cycle analysis of the driving-force system of the climate evolution

Previous studies have shown that the Neogene coal seams contain information related to Milankovitch cycles. The information regarding these cycles can be found using spectrum analysis methods, as well as other signals, which allow for the paleoclimate cycles in coal seams to be examined^[71-72]. In this study, using the results of the spectrum analysis, and by processing the available logging data (natural gamma and rock density logging data) of the No. 4 coal seam of the Yan 1 Section in the Binchang Coal Field, the Earth's orbiting parameters were successfully determined and Milankovitch cycle was identified. Therefore, the number and average thicknesses of the paleoclimate cycles formed by the Earth's orbiting parameters in the No. 4 coal seam could be analyzed. The obtained results illuminated the development mechanism of the paleoclimate cycles from the perspective of their genetic mechanism, and then verified the reliability of the paleoclimate cycles which had been comprehensively identified using the above-mentioned four methods. Then, by utilizing the results of the one-dimensional continuous wavelet transform analysis of the natural gamma and rock density logging data of the No. 4 coal seam of the Yan 1 Section in the Binchang Coal Field previously completed by Wang et al. (2018), the average values of the low-frequency, medium-frequency, and high-frequency were determined to be 0.28 cycle/m, 0.65 cycle/m, and 1.33 cycle/m, respectively, as identified by the spectrum analysis. Then, the Milankovitch cycles contained therein were identified^[58]. The Milankovitch cycles controlled by the different orbital parameters in the No. 4 coal seam were further classified as follows: Four long-term cycles controlled by eccentricity; nine middle-term cycles controlled by gradient; and fifteen short-term cycles controlled by precession. It was considered that the paleoclimate cycles in the No. 4 coal seam of the Yan 1 Section were astronomical cycles controlled by eccentricity.

In summary, it was confirmed in this study that approximately four periodic cycles of climate change controlled by eccentricity cycles had occurred during the formation of the No. 4 coal seam of the Yan 1 Section. Additionally, it was found that the content levels of inertinite were higher during the dry climate periods.

5.2 Relationship between the Free Radical Concentrations of the Inertinite and the Genesis Temperature of the Coal

Austen et al. [31] suggested that the concentrations of free radicals varied very little before the highest temperature had ever been experienced by organic matter during its history [31]. Zhuang and Wu et al. (1996) conducted a paramagnetic resonance study of the fusain in the No. 4 coal seam of the Yan 1 Section in the Binchang Coal Field [25], and determined that the free radical concentrations of fusain in the coal seam had changed significantly with the increases in temperature. It was found that the temperature point which had shown the most obvious change was approximately 300 °C, which indicated that the highest temperature of the fusain during the entire coal gasification process had not exceeded 300 °C. It could be seen from the curve shape of the relationship between the heating temperature and the concentrations of free radicals that the curve shapes of the fusain and oxidized wood were very similar. For example, an obvious prominent double peak type was seen, which was significantly different from the “front flat and rear steep” single peak shapes of the destructive distilled charcoal (Figure 7a). A similar conclusion could be drawn from the curve shapes of the relationship between the heating temperature of the dull coal and the concentrations of free radicals (Figure 7b). Therefore, Zhuang and Wu [25] put forward the theory that the fusain in the No. 4 coal seam of the Yan 1 Section of the Binchang Coal Field had not been formed by burning actions, but were instead related to the strong putrefaction and biochemical oxidation during the early formation stages of the peat [25]. However, the oxidation could not be separated from the participation of the microorganisms. The activities of the microorganisms had been mainly restricted by the surrounding environmental conditions. Therefore, under the conditions of sufficient available nutrients, the most important factor would be temperature. The suitable temperature range for microbial activities is known to be between 0 and 80 °C. It has been observed that under the conditions of atmospheric pressure, microorganism tend to be the most physiologically active in the temperature range of 30 to 50 °C [73]. This study’s simulation results revealed that the maximum temperature of the fusain during the entire coalification process had not

exceeded 300 °C, which was too high for microorganisms, and not conducive to microorganism activities or the formation of inertinite.

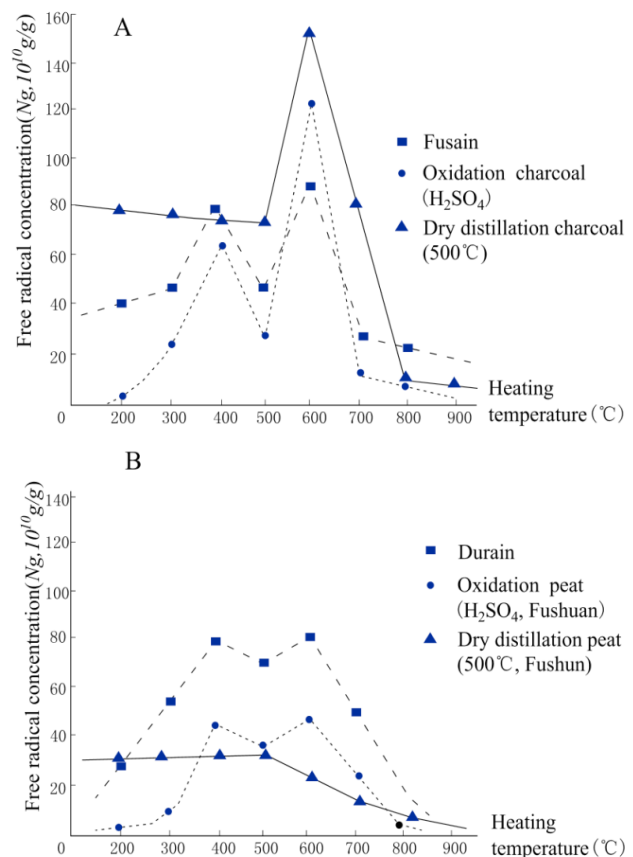


Figure 7. Relation schema between heating temperature and free radical concentration [25]

5.3 Relationship between the Types and Temperature Levels of the Wildfires and the Reflectance of the Inertinite

By the late Silurian Period, plants occupied large portions of the Earth’s surface, and the oxygen content in the atmosphere had reached levels which could maintain wildfire events (> 15%). As a result, wildfire events often occurred. During the deposition period of the Middle Jurassic Yan’an Formation, the oxygen concentrations in the atmosphere were known to have exceeded 15% (Figure 8), and the basic conditions for wildfire events were available.

As detailed in Table 4, wildfires can be grouped [29] as follows: (1) Ground fires burning organic material below the litter level, (2) Surface fires burn litter and herbaceous and shrub type plants; and (3) Crown fires burning the canopy of trees and larger shrubs. The fire types are also characterized by different burning temperature levels, with ground fires producing temperatures of approximately

300 °C . However, the flames in many such fires generally produce temperatures of approximately 600 °C . Moreover, intense temperatures of 800 °C or higher can potentially be reached in crown fires (for example, in stands of conifers) [35, 74].

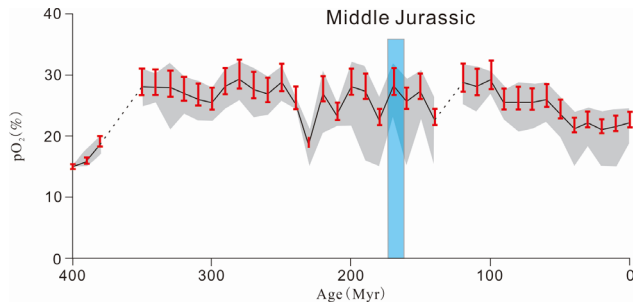


Figure 8. Prediction of pO_2 from Inert%. Line; best estimate based on late Palaeozoic pO_2 maxima of 30%. Error bars 1 s.d. from mean. Shaded area; estimate of maximum error assuming Phanerozoic pO_2 maxima of 35% + 1 s.d. (upper margin) and 25% % 1 s.d. (lower margin) [75]

The correlation between inertinite reflectance and the burning temperature range is not completely linear. The correlation can be described by the linear regression equation $T = 184.10 + 117.76 \times \%R^o$ ($r^2 = 0.91$), where T is the burning temperature and $\%R^o$ indicates the measured inertinite reflectance [76].

In the present study, according to the reflectance test results of the inertinite in the No. 4 coal seam of the Yan 1 Section of the Binchang Coal Field (Table 3), the minimum reflectance of the coal was 0.91%, and its formation temperature was 291.3 °C . The maximum reflectance was determined to be 2.53%, and its corresponding temperature was 482 °C . In addition, the reflectance of individual points was 4.54%, and the corresponding temperature was 718.7 °C . For the nine examined samples obtained from the study area, the average reflectance of the inertinite ranged between 1.35 and 1.79%, and the corresponding temperature range was between 354.9 and 394.9 °C . This study’s calculation results showed that the genesis of the wildfire events in the No. 4 coal seam of the Yan 1 Section in the study area were mainly ground fires, and partially surface fires (Table 4). Furthermore, the calculated results showed that the temperature range was similar to the fusain formation temperatures measured by Zhuang and Wu [25].

Ground fire is a type of fire with low combustion intensity, long duration, and strong concealment characteristics. This type of fire event often occurs in the humus and peat layers of forests and wetlands. During the dry seasons, ground fire events occur throughout world and are affected by climate changes and extreme weather conditions [77]. The occurrences of ground fire events are very common.

The rich near-soil layers and underground combustibles form the material conditions for the occurrences of ground fire events. In the cases of low precipitation, long-term drought, increased ground temperatures, decreased relative humidity, and the drying of combustible material, surface fires and lightning can potentially result in ground fires. Ground fires generally burn slowly, last for a long time, burn insufficiently, and have the characteristics of strong concealment, combustion discontinuity, and variable direction [79]. Ground fire events have geographical and temporal distribution characteristics. Also, when compared with humus, peat is the main limiting factor of the spatial distributions of ground fires. Approximately 80% of peat is distributed in northern temperate zones, 15% to 20% in the tropical and subtropical zones, and only a small percentage is distributed in southern temperate zones [79]. In regard to time distributions, ground fires generally occur during dry seasons [77].

Table 4. Inertinite reflectance populations and assumed burning temperatures [36]

Stage	-0.70-2.10% R_o -250-400 °C	-2.10-3.30% R_o -400-550 °C	-3.30-4.10% R_o -550-650 °C	>4.10% R_o -650 ->800 °C	Included beds
upper Sinemurian	a 8%	8%	2%	1%	Galgelokke
	b 1.39% R_o	2.57% R_o	3.59% R_o	4.83% R_o	
	c 348 °C	487 °C	607 °C	753 °C	
lower Sinemurian	a 79-97%	3-16%	0-4%	0-2%	Oresund-18 Sose Bugt B
	b 1.25-1.54% R_o	2.47-2.49% R_o	3.51% R_o	4.73% R_o	
	c 331-365 °C	475-477 °C	597 °C	741 °C	
Hettangian	a 83-98%	3-14%	0-2%	0-1%	Sose Bugt D Oresund-13 Munkerup
	b 1.26-1.56% R_o	2.41-2.67% R_o	3.72-3.89% R_o	4.73-5.29% R_o	
	c 332-368 °C	468-499 °C	622-642 °C	741-807 °C	
Rhaetian (A-bed)	a 94%	6%	0%	0%	Norra Albert
	b 1.44% R_o	2.26% R_o	-	-	
	c 354 °C	450 °C	-	-	
Rhaetian (B-bed)	a 61-73%	16-21%	7-11%	5%	Norra Albert Lunnon Billesholm
	b 1.39-1.43% R_o	2.52-2.57% R_o	3.64-3.70% R_o	4.52-4.95% R_o	
	c 349-352 °C	481-487 °C	613-620 °C	716-767 °C	
Fire type	Ground/surface fire		Surface fire	Crown fire	

^aPercentage of all measurements. Range indicates average of different beds
^bAverage inertinite reflectance of selected population. Range indicates average of different beds
^cEstimated burning temperature (T) range based on the equation $T = 184.10 + 117.76 \times \%R_o$

Figure 5. Inertinite reflectance populations and assumed burning temperatures. High-reflecting inertinite corresponding to temperatures >600 °C that can be obtained in crown fires of stands of conifers is particularly abundant in the Rhaetian B-bed.

High-reflecting inertinite corresponding to temperatures >600 °C that can be obtained in crown fires of stands of conifers is particularly abundant in the Rhaetian B-bed.

Using experimental simulation methods, Wang et al. (2018) found that the critical point temperature of peat transformation from self-heating to spontaneous combustion was approximately 50 °C [80]. That is to say, the external conditions must make the internal temperature of peat reach above 50 °C in order to maintain the self-heating and spontaneous combustion reactions of the peat. It was believed in this study that the southern Ordos Basin was located near a northern temperate zone during the Middle Jurassic Period, during which time the climate of Yan’an Formation had been relatively dry. This had provided the necessary conditions for the development of ground fires. Therefore, inertinite formation in the coal seam may have resulted from wildfire events.

6. Conclusions

Through the above-mentioned analysis results, the following cognition was obtained:

(1) During the formation period of the No. 4 coal seam of the Yan 1 Section in the southern section of the Ordos Basin, the overall climate had been relatively dry. It was determined that four cycles with alternating dry and wet climate conditions controlled by the eccentricity astronomical period had occurred. During the dry climate periods, the content of inertinite was relatively high.

(2) The formation of inertinite by oxidation could not be separated from the participation of the microorganisms, and the temperature range known to be suitable for microorganisms activity is between 0 and 80 °C. This study's simulation results of the free radical concentrations showed that the maximum temperature of the fusain in the No. 4 coal seam of the Yan 1 Section in the study area had not exceeded 300 °C. However, this was too high for microorganism activities, and also not conducive to the formation of inertinite.

(3) It was found in this study that, according to the calculation results of the reflectance of inertinite, the genesis temperature of the inertinite had been lower than 400 °C. These findings indicated that the wildfire type genesis of the No. 4 coal seam in the Yan 1 Section in the study area had been mainly ground fire, and partially surface fire. Moreover, the geographical location, climatic conditions, atmospheric oxygen concentration, and so on of the study area were all conditions favorable for the occurrences of wildfire event. Therefore, it was speculated in this study that there was also inertinite of oxidation genesis in the study area. However, this had not been the main genesis type.

(4) There were dense and scattered fusinite observed in the No. 4 coal seam of the Yan 1 Section in the study area, and the thicknesses of the cell walls were observed to be different. It was speculated that these differences were related to the wildfire type, combustion temperature, combustion time, and the different initial conditions of the combusted objects during the coal forming periods.

References

- [1] Stach E., Mackowsky M. T., Teichmüller M, et al. Stach's Textbook of Coal Petrology, 3rd Ed [M]. Gebrüder Borntraeger, Berlin, 1982, 535.
- [2] Taylor G. H., Liu S. Y. and Diessel C. F. K. The Cold-climate Origin of Inertinite-rich Gondwana Coals [J]. *International Journal of Coal Geology*, 1989, 11(1): 1-22
- [3] Singh M. P. and Shukla R. R. Petrographic Characteristics and Depositional Conditions of Permian Coals of Pench, Kanhan, and Tawa Vally Coalfields of Satpura Basin, Madhya Pradesh, India [J]. *International Journal of Coal Geology*, 2004, 59: 209–243.
DOI: 10.1016/0166-5162 (89)90110-9
- [4] Li X. Y. Conditions of Inertinite-rich Coal Generation, Shendong Mining area: Significance of Fungal Alternating Origin of Inerts [J]. *Coal Geology & Exploration*, 2005, 33(5): 1-4.
DOI: 10.1016/j.coal.2004.02.002
- [5] Jasper A., Uhl D., Guerra-Sommer M, et al. Upper Paleozoic Charcoal Remains from South America: Multiple Evidences of fire events in the Coal bearing Strata of the Paraná Basin, Brazil [J]. *Palaeogeography, Palaeoclimatology, Palaeoecology*, 2011, 306: 205–218.
DOI: 10.1016/j.palaeo.2011.04.022
- [6] Jasper A., Guerra-Sommer M., Hamad A. M. B. A., et al. The Burning of Gondwana: Permian fires on the Southern Continent — A palaeobotanical Approach [J]. *Gondwana Research*, 2013, 24: 148-160.
DOI: 10.1016/j.gr.2012.08.017
- [7] Jasper A., Agnihotri D., Tewari R, et al. Fires in the mire: Repeated fire events in Early Permian 'peat forming' Vegetation of India [J]. *Geological Journal*, 2016, 52: 955-969.
DOI: 10.1002/gj.2860
- [8] Manfroi J., Uhl D., Guerra-Sommer M, et al. Extending the database of Permian palaeowildfire on Gondwana: Charcoal remains from the Rio do Rasto Formation (Paraná Basin), Middle Permian, Rio Grande do Sul State, Brazil [J]. *Palaeogeography, Palaeoclimatology, Palaeoecology*, 2015, 436: 77–84.
DOI: 10.1016/j.palaeo.2015.07.003
- [9] Kauffmann M., Jasper A., Uhl D, et al. Evidence for palaeowildfire in the Late Permian palaeotropics — Charcoal from the Motuca Formation in the Paraná Basin, Brazil [J]. *Palaeogeography, Palaeoclimatology, Palaeoecology*, 2016, 450: 122–128.
DOI: 10.1016/j.palaeo.2016.03.005
- [10] Wu C. R., Zhang H., Li X. Y, et al. Study on Coal Quality and Coal Metamorphism of Early-Middle Jurassic Coal Rocks in Northwest China [M]. Beijing: Coal Industry Press, 1995.
- [11] Zhang X. Y., Tong Y. Z., Xiao D. X, et al. Discussion on the Genesis of Huangling Candle Coal [J]. *Coalfield Geology of China*, 1996(S): 10-16.
- [12] Zhang J., Yu B. and Tang J. X. Characteristics and

- Facies of Ya-8 coal in Yining Coalfield, Xinjiang [J]. *Coalfield Geology of China*, 1999, 11(1): 30–32.
- [13] Li W. H., Chen Y. F., Chen W. M., et al. Distribution Features of Micro-Constituents for Coal in China Main Mining Area [J]. *Coal Science and Technology*, 2000, 28(9): 31–34.
DOI: 10.13199/j.cst.2000.09.34.liwh.011
- [14] Zeng F. G. Petrographic Characteristics of Coal Seam No2-2 from Daliuta mine district, Shenfu area, North Shaanxi [J]. *Coal Geology & Exploration*, 2000, 28(3): 25–27. Bai X. F., Li W. H., Chen W. M., et al. Study on Distribution and Characteristics of coals with weak reductive degree in West china[J]. *Journal of Coal Science*, 2005, 30(4): 502–506.
DOI: 10.13225/j.cnki.jccs.2005.04.021
- [15] Chang H. Z., Zeng F. G., Li W. Y., et al. Micro-FTIR Study on Structure of Macerals from Jurassic Coals in Northwestern China [J]. *Spectroscopy and Spectral Analysis*, 2008, 28(7): 1535-1539.
DOI: 10.1016/j.sab.2008.04.017
- [16] Huang W. H., Tang S. H., Tang X. Y., et al. The Jurassic coal petrology and the research significance of Northwest China [J]. *Coal Geology & Exploration*, 2010, 38(4): 1-6.
DOI: 1001-1986 (2010) 04-0001-06
- [17] Hower J. C., O’Keefe J. M. K., Watt M. A., et al. Notes on the origin of inertinite macerals in coals: Observations on the importance of fungi in the origin of macrinite [J]. *International Journal of Coal Geology*, 2009, 80(2): 135–143.
DOI: 10.1016/j.coal.2009.08.006
- [18] Hower J. C., O’Keefe J. M. K., Volk T. J., et al. Funginite-resinite associations in coal [J]. *International Journal of Coal Geology*, 2010, 83(1): 64-72.
DOI: 10.1016/j.coal.2010.04.003
- [19] Teichmüller M. Vergleichende mikroskopische Untersuchungen versteinertes Torfies des Ruhrkarbons und der daraus entstanden Steinkohlen [C]. C. R., 3rd Carboniferous Cong, Heerlen, 1952: 607-613.
- [20] Han D. X. Coal petrology in China [M]. Shanghai: East China Normal University Press, 1996.
- [21] Harvey R. D. and Dillon J. W. Maceral distributions in Illinois coals and their paleoenvironmental implications [J]. *International Journal of Coal Geology*, 1985, 5(1-2): 141-165.
DOI: 10.1016/0166-5162(85)90012-6
- [22] Phillips T. L., Peppers R. A. and Dimichele W. A. Stratigraphic and interregional changes in Pennsylvanian coal-swamp vegetation: Environmental inferences[J]. *International Journal of Coal Geology*, 1985, 5(1-2): 43-109.
DOI: 10.1016/0166-5162(85)90010-2
- [23] Hunt J. W. and Smyth M. Origin of Inertinite-rich coals of Australian Cratonic Basins [J]. *International Journal of Coal Geology*, 1989, 11(1): 23-46.
DOI: 10.1016/0166-5162(89)90111-0
- [24] Zhuang J. and Wu J. J. Middle Jurassic coal accumulation characteristics and coal comprehensive utilization of southern Ordos Basin [M]. Beijing: Geological Publishing House, 1996.
- [25] Chen X. W., Zhuang X. G., Zhou J. B., et al. Coal Quality and its Distribution of the Eastern Junggar Coalfield in Junggar Basin, Xinjiang [J]. *Xinjiang Geology*, 2013, 31(1): 89-94.
DOI: 10.3969/j.issn.1000-8845.2013.01.019
- [26] Hagelskamp H. H. B. and Snyman C. P. On the Origin of Low-reflecting Inertinites in Coals from the Highveld Coalfield, South Africa [J]. *Fuel*, 1988, 67(3): 307-313.
DOI: 10.1016/0016-2361(88)90311-0
- [27] Moore T. A., Shearer J. C. and Miller S. L. Fungal origin of oxidised plant material in the Palangkaraya peat deposit, Kalimantan Tengah, Indonesia: Implications for ‘inertinite’ formation in coal [J]. *International Journal of Coal Geology*, 1996, 30(1-2): 1-23.
DOI: 10.1016/0166-5162(95)00040-2
- [28] Styan W. B. and Bustin R. M. Petrography of some Fraser river delta peat deposits: Coal maceral and microlithotype precursors in temperate-climate peats [J]. *International Journal of Coal Geology*, 1983, 2(4): 321-370.
DOI: 10.1016/0166-5162(83)90016-2
- [29] Scott A. C. Observation on the nature and origin of fusinite [J]. *International Journal of Coal Geology*, 1989, 12(1-4): 443-475.
DOI: 10.1016/0166-5162(89)90061-X
- [30] Teichmüller M. The genesis of coal from the viewpoint of coal petrology [J]. *International Journal of Coal Geology*, 1989, 12(1-4): 1-87.
DOI: 10.1016/0166-5162(89)90047-5
- [31] Austen D. E. G., Ingram D. J. E., Given P. H., et al. Electron spin resonance study of pure macerals[J]. *Coal Science*, 1966, 55: 344-362.
DOI: 10.1021/ba-1966-0055.ch021
- [32] Jones T. P. and Chaloner W. G. Fossil charcoal, its recognition and palaeoatmospheric significance [J]. *Palaeogeography, Palaeoclimatology, Palaeoecology*, 1991, 97(1-2): 39-50.
DOI: 10.1016/0031-0182(91)90180-Y
- [33] Bustin R. M. and Guo Y. Abrupt changes (jumps) in reflection values and chemical compositions of artificial charcoals and inertinite in coals[J]. *International Journal of Coal Geology*, 1999, 38(3-4): 237-

260.
DOI: 10.1016/ S0166-5162(98) 00025-1
- [34] Guo Y. and Bustin R. M. FTIR spectroscopy and reflectance of modern charcoals and fungal decayed woods: implications for studies of inertinite in coals[J]. *International Journal of Coal Geology*, 1998, 37(1-2): 29-53.
DOI: 10.1016/ S0166-5162(98) 00019-6
- [35] Scott A. C. The Pre-Quaternary history of fire [J]. *Palaeogeography, Palaeoclimatology, Palaeoecology*, 2000, 164: 281-329.
DOI: 10.1016/ s0031-0182(00) 00192-9
- [36] Petersen H. I. and Lindström S. Synchronous Wildfire Activity Rise and Mire Deforestation at the Triassic–Jurassic Boundary [J]. *Plos One*, 2012, 7(10): e47236.
DOI: 10.1371/ journal. pone. 0047236
- [37] Uglík M. and Nowak J. L. Petrological recognition of bituminous inertinite enriched coals of the Lower Silesian Coal Basin (Central Sudetes, SW Poland) [J]. *International Journal of Coal Geology*, 2015, 139: 49–62.
DOI: 10.1016/j.coal.2014.07.009
- [38] Wang Z. Q. and Chen A. S. Traces of arborescent lycopsids and dieback of the forest vegetation in relation to the terminal Permian mass extinction in North China [J]. *Review of Palaeobotany and Palynology*, 2001, 117: 217–243.
DOI: 10.1016/ S0034 -6667(01) 00094-X
- [39] Sun Y. Z., Püttmann W., Kalkreuth W, et al. Petrologic and geochemical characteristics of seam 9–3 and Seam 2, Xingtai Coalfield, northern China [J]. *International Journal of Coal Geology*, 2002, 49: 251–262.
DOI: 10.1016/ S0166-5162(01) 00067-2
- [40] Yan M. X., Wan M. L., He X. Z., et al. First report of Cisuralian (early Permian) charcoal layers within a coal bed from Baode, North China with Reference to Global Wildfire Distribution [J]. *Palaeogeography, Palaeoclimatology, Palaeoecology*, 2016, 459: 394–408.
DOI: 10.1016/j.palaeo.2016.07.031
- [41] Sun Y. Z., Zhao C. L., Püttmann W, et al. Evidence of widespread wildfires in a coal seam from the middle Permian of the North China Basin [J]. *Lithosphere*, 2017, 9(4): 595-608.
DOI: 10.1130/L638.1
- [42] Uhl D. and Kerp H. Wildfires in the late Palaeozoic of Central Europe—The Zechstein (Upper Permian) of NW-Hesse (Germany) [J]. *Palaeogeography, Palaeoclimatology, Palaeoecology*, 2003, 199: 1–15.
DOI: 10.1016/ S0031-0182(03) 00482-6
- [43] Noll R., Uhl D. and Lausberg S. Brandstrukturen an Kieselhölzern der Donnersberg Formation (Oberes Rotliegend, Unterperm) des Saar-Nahe-Beckens (SW-Deutschland) [J]. *Veröffentlichungen des Museums für Naturkunde Chemnitz*, 2003, 26: 63–72.
- [44] Uhl D., Lausberg S., Noll R, et al. Wildfires in the late Palaeozoic of central Europe — An overview of the Rotliegend (Upper Carboniferous–Lower Permian) of the Saar-Nahe Basin (SW-Germany) [J]. *Palaeogeography, Palaeoclimatology, Palaeoecology*, 2004, 207(1-2): 23–35.
DOI: 10.1016/ j.palaeo. 2004.01.019
- [45] Uhl D., Jasper A., Hamad A. M. B, et al. Permian and Triassic wildfires and atmospheric oxygen levels [C]. *Proceedings, 1st WSEAS International Conference on Environmental and Geological Science and Engineering: World Scientific and Engineering Academy and Society*, 2008: 179–187.
- [46] Uhl D., Butzmann R., Fischer T. C, et al. Wildfires in the late Palaeozoic and Mesozoic of the Southern Alps — The late Permian of the Bletterbach-Butterloch area (northern Italy) [J]. *Rivista Italiana di Paleontologia e Stratigrafia*, 2012, 118(2): 223–233.
DOI:10.13130/ 2039-4942/ 6002
- [47] Scott A. C. Coal petrology and the origin of coal macerals: a way ahead [J]. *International Journal of Coal Geology*, 2002, 50(1-4): 119-134.
DOI: 10.1016/ S0166-5162(02) 00116-7
- [48] Scott A. C. and Glasspool I. J. Observations and Experiments on the Origin and Formation of Inertinite Group Macerals [J]. *International Journal of Coal Geology*, 2007, 70(1-3): 53-66.
DOI: 10.1016/ j.coal. 2006.02.009
- [49] Diessel C. F. K. The Stratigraphic Distribution of Inertinite[J]. *International Journal of Coal Geology*, 2010, 81(4): 251–268.
DOI: 10.1016/ j.coal. 2009. 04. 004
- [50] Wang D. D. Sequence-palaeogeography and Coal-accumulation of the Middle Jurassic Yan’an Formation in Ordos Basin [D]. Beijing: China University of Mining and Technology, 2012: 224-225.
- [51] Vakhrameev V. A. Range and Paleocology of Mesozoic Conifers, Cheirolepidiaceae [J]. *Paleontological Journal*, 1970, 70(1): 19-34.
- [52] Miao S. J. Spore pollen, Mesozoic Strata and Paleontology in the Coal bearing Strata of Guyang, Inner Mongolia [M]. Beijing: Geological Publishing House, 1982.
- [53] Duan Z. H. Classopollis pollen and its paleoclimate meaning[J]. *Coal Geology and Exploration*, 1991, 19(6): 14-21.
- [54] Qian. L. J. and Wu J. J. The Jurassic Spore pollen

- Combination in the Northwestern Shaanxi, The Jurassic Coal-bearing Strata and coal Accumulation Characteristics in the Northwestern Shaanxi [M]. Xi'an: Northwest University Press, 1987.
- [55] Zhou C. G., Yang Q., Pan Z. G, et al. Paleo-climate Evolution of Yan'an Stage Inferred from Petrographic Composition of Coal [J]. *Coal Geology of China*, 1996, 8(4): 12-14+19.
- [56] Yang Q. and Han D. X. *Coalfield Geology of China* [M]. Beijing: Coal Industry Press, 1979.
- [57] Wang D. D., Yan Z. M., Liu H. Y, et al. The net primary productivity of Mid-Jurassic peatland and its control factors: Evidenced by the Ordos Basin [J]. *International Journal of Mining Science and Technology*, 2018, 28(2): 177-185.
DOI: org/ 10.1016/ j.ijmst. 2017.06.001
- [58] Fang A. M., Lei J. J., Jin K. L, et al. An Anthracographic Study on No.7 Coal in Xishan Coalfield, Shanx [J]. *Coal Geology of China*, 2003, 15(5): 12-16.
- [59] Wang D. Z. A Study on No.5 Coal Seam Facies, Huating Mining Area [J]. *Coal Geology of China*, 2005, 17(4): 6-8+70.
DOI: 10.3969/ j.issn. 1674-1803. 2005.04.003
- [60] Li Q. Coal facies of No.2 coal in Yanchuannan coal field of Shanxi: Significance for constituencies of coalbed methane exploitation [J]. *Petroleum Geology & Experiment*, 2014, 36(2): 245-248+256.
DOI: 10.11781/ sysydz 201402245
- [61] Fan Y. H., Qu H. J., Wang H, et al. The application of trace elements analysis to identifying sedimentary media environment: a case study of Late Triassic strata in the middle part of western Ordos Basin [J]. *Geology in China*, 2012, 39(2): 382-389.
DOI: 10.1016/ j.still. 2012.05.017
- [62] Wang S. J., Huang X. Z., Tuo J. C, et al. Evolutional Characteristics and Their Paleoclimate Significance of Trace Elements in the Hetaoyuan Formation, Biyang Depression [J]. *Acta Sedimentologica Sinica*, 1997, 15(1): 66-71.
DOI: 10.14027/ j.cnki.cjxb. 1997.01.012
- [63] Hu X. F., Liu Z. J., Liu R, et al. Trace Element Characteristics of Eocene Jijuntun Formation and the Favorable Metallogenic Conditions of Oil Shale in Fushun Basin [J]. *Journal of Jilin University(Earth Science Edition)*, 2012, 42(S1): 60-71.
DOI: 10.13278/ j.cnki.jjuese. 2012.s1.008
- [64] Zhang B. and Yao Y. M. Trace Element and Palaeoenvironmental Analyses of the Cenozoic Lacustrine Deposits in the Upper Es4 Submember of the Dongying Basin [J]. *Journal of Stratigraphy*, 2013, 37(2): 186-192.
- [65] Teng G. R., Liu W. H., Xu Y. C, et al. The Discussion on Anoxic Environments and Its Geochemical Identifying Indices [J]. *Acta Sedimentologica Sinica*, 2004, 22(2): 365-372.
DOI: 10.3969/ j.issn. 1000- 0550. 2004.02.026
- [66] Liang W. J., Xiao C. T. and Xiao S. Study on Relationships between Palaeoenvironment, Palaeoclimate of Middle Permian-middle Triassic and Constant, Trace Elements in Western Sichuan [J]. *Science Technology and Engineering*, 2015, 15(11): 14-24.
- [67] Zhao X. W. *Introduction to Paleoclimatology* [M]. Beijing: Geological Publishing House, 1992.
- [68] Lu J., Shao L. Y., Wang Z. G, et al. Organic carbon isotope composition and paleoclimatic evolution of Jurassic coal seam in the northern Qaidam basin [J]. *Journal of China University of Mining & Technology*, 2014, 43(4): 612-618.
DOI: 10.13247/ j.cnki.jcmt. 000091
- [69] Lu J., Yang M. F., Shao L. Y, et al. Paleoclimate change and sedimentary environment evolution, coal accumulation: A Middle Jurassic terrestrial [J]. *Journal of China Coal Society*, 2016, 41(7): 1788-1797.
DOI: 10.13225/ j.cnki.jccs. 2016. 0061
- [70] Large D. J. A 1.16 Ma record of carbon accumulation in western European peatland during the Oligocene from the Ballymoney lignite, Northern Ireland [J]. *Journal of the Geological Society*, 2007, 164(6): 1233-1240.
DOI: 10.1144/ 0016-76492006-148
- [71] Large D. J., Jones T. F., Somerfield C, et al. High-resolution Terrestrial Record of Orbital Climate Forcing in Coal [J]. *Geology*, 2003, 31(4): 303-306.
DOI: 10.1130/ 0091-7613 (2003)031 <0303: HR-TROO> 2.0.CO;2
- [72] Li X. Q., Zhang S. C., Zhu G. Y, et al. Types and Research Direction of Biogenic Gas in China [J]. *Natural Gas Geoscience*, 2005, 16(4): 477-484.
- [73] Scott A. C. and Jones T. P. The Nature and Influence of fire in Carboniferous Ecosystems [J]. *Palaeogeography, Palaeoclimatology, Palaeoecology*, 1994, 106(1-4): 91-112.
DOI: 10.1016/ 0031-0182 (94) 90005-1
- [74] Glasspool I. J. and Scott A. C. Phanerozoic Concentrations of Atmospheric Oxygen Reconstructed from Sedimentary Charcoal [J]. *Nature Geoscience*, 2010, 3(9): 627-630.
DOI: 10.1038/ ngeo923
- [75] Jones T. P. Fusain in Late Jurassic Sediments from Witch Ground Graben, North Sea [J]. *U.K, Mededelingen Nederlands Instituut voor Toegepaste Ge-*

- owetenschappen TNO, 1997, 58: 93–103.
- [76] Zhang J. L. and Di X. Y. The Study of Ground Fire and Smoldering: A Review [J]. *Journal of Temperate*, 2018, 1(3): 19-23.
DOI: 10.3969/j.issn.2096-4900.2018.03.004
- [77] Shu L. F., Wang M. Y., Tian X. R., et al. Fire Environment Mechanism of Ground fire Formation in Daxing' an Mountains [J]. *Journal of Natural Disasters*, 2003, 12(4): 62-68.
DOI: 10.13577/j.jnd.2003.0411
- [78] Rein G., Cleaver N., Ashton C, et al. The Severity of Smouldering Peat Fires and Damage to the Forest Soil [J]. *Catena*, 2008, 4(3): 304-309.
DOI: 10.1016/j.catena.2008.05.008
- [79] Wang H. R., Liang D., Zhan G. T, et al. Spontaneous Combustion Characteristics of Peat under Low Temperature [J]. *Fire Science and Technology*, 2018, 37(2): 171-174.
DOI: 10.3969/j.issn.1009-0029.2018.02.007